

**Structural anomalies and the orbital ground state in FeCr<sub>2</sub>S<sub>4</sub>**V. Tsurkan,<sup>1,2</sup> O. Zaharko,<sup>3</sup> F. Schrettle,<sup>1</sup> Ch. Kant,<sup>1</sup> J. Deisenhofer,<sup>1</sup> H.-A. Krug von Nidda,<sup>1</sup> V. Felea,<sup>2,4</sup> P. Lemmens,<sup>4</sup> J. R. Groza,<sup>5</sup> D. V. Quach,<sup>5</sup> F. Gozzo,<sup>6</sup> and A. Loidl<sup>1</sup><sup>1</sup>*Experimental Physics 5, Center for Electronic Correlations and Magnetism Institute of Physics, University of Augsburg, 86159 Augsburg, Germany*<sup>2</sup>*Institute of Applied Physics, Academy of Sciences of Moldova, MD-2028 Chisinau, Republic of Moldova*<sup>3</sup>*Laboratory for Neutron Scattering, ETHZ and PSI, CH 5232 Villigen, Switzerland*<sup>4</sup>*Institute for Condensed Matter Physics, TU Braunschweig, D-38106 Braunschweig, Germany*<sup>5</sup>*Department of Chemical Engineering and Materials Science, University of California, Davis, California 95616, USA*<sup>6</sup>*Swiss Light Source, PSI, CH 5232 Villigen, Switzerland*

(Received 22 December 2009; revised manuscript received 28 April 2010; published 21 May 2010)

We report on high-resolution x-ray synchrotron powder-diffraction, magnetic-susceptibility, sound-velocity, thermal-expansion, and heat-capacity studies of the stoichiometric spinel FeCr<sub>2</sub>S<sub>4</sub>. We provide clear experimental evidence of a structural anomaly which accompanies an orbital-order transition at low temperatures due to a static cooperative Jahn-Teller effect. At 9 K, magnetic susceptibility, ultrasound velocity, and specific heat reveal pronounced anomalies that correlate with a volume contraction as evidenced by thermal-expansion data. The analysis of the low-temperature heat capacity using a mean-field model with a temperature-dependent gap yields a gap value of about 18 K and is interpreted as the splitting of the electronic ground state of Fe<sup>2+</sup> by a cooperative Jahn-Teller effect. This value is close to the splitting of the ground state due to spin-orbit coupling for isolated Fe<sup>2+</sup> ions in an insulating matrix, indicating that Jahn-Teller and spin-orbit coupling are competing energy scales in this system. We argue that due to this competition, the spin-reorientation transition at around 60 K marks the onset of short-range orbital ordering accompanied by a clear broadening of Bragg reflections, an enhanced volume contraction compared to usual anharmonic behavior, and a softening of the lattice observed in the ultrasound measurements.

DOI: [10.1103/PhysRevB.81.184426](https://doi.org/10.1103/PhysRevB.81.184426)

PACS number(s): 75.25.Dk, 75.40.-s, 75.50.Gg

**I. INTRODUCTION**

During the last decade, orbital physics evolved as a fascinating topic in modern solid-state physics and materials science. The spatial orientation of the electronic orbitals governs magnetic exchange and, hence, determines long-range spin order. If the orientational order of orbitals can be changed by external fields, e.g., lattice strain, the magnetic order will change concomitantly. On long terms such a targeted tuning of electronic orbitals, so-called orbitronics, could be an important ingredient of a future correlated-electron technology.<sup>1</sup> Orbital-ordering phenomena in solids are well established. Usually strong electron-phonon coupling lifts the orbital degeneracy and results in a long-range orbital order (OO) and in a concomitant lowering of the crystal symmetry via the time-honored Jahn-Teller (JT) effect.<sup>2,3</sup> In electronically strongly correlated systems, OO may also be established by the Kugel-Khomskii mechanism<sup>4</sup> where the orbital degeneracy is removed via a purely electronic interaction.

The cooperative JT effect has predominantly been studied in rare-earth systems and in transition-metal oxides and sulfides, mainly in spinels and perovskite systems.<sup>3</sup> In normal spinels with the general formula AB<sub>2</sub>X<sub>4</sub>, where A and B are transition metals and X=O, S, or Se, the crystal structure is cubic (*Fd* $\bar{3}m$ ) with 8 f.u. per unit cell. In these compounds, the oxygen or chalcogenide ions form a face-centered-cubic network in which the A ions occupy 1/8 of the tetrahedral and 1/2 of, the B ions, the octahedral sites, respectively. The JT effect can arise either from the A sites or from the B sites,

or from both simultaneously. The onset of long-range magnetic order, if being established, usually is associated with the transition-metal ion on the B site because of the dominating B-B exchange coupling (i.e., direct B-B exchange in oxide spinels and B-X-B superexchange in sulfide and selenide spinels). In case of FeCr<sub>2</sub>S<sub>4</sub>, the non-JT-active Cr ion is the driving force establishing spin order.

In FeCr<sub>2</sub>S<sub>4</sub>, the Cr sublattice (Cr<sup>3+</sup>: electronic configuration 3d<sup>3</sup>, S=3/2) at the B sites is dominated by a ferromagnetic (FM) exchange via the 90° Cr-S-Cr bond angle. The low-lying t<sub>2g</sub> triplet in octahedral symmetry is half filled and the orbital moment is quenched. The Fe ions (Fe<sup>2+</sup>: 3d<sup>6</sup>, S=2) are located at the tetrahedrally coordinated A sites. In this case, the fivefold-degenerate ground state is split by the crystal field into a lower orbital doublet and an excited triplet. In the magnetically ordered state, the exchange field further splits the spin degeneracy of the e doublet into 2S+1=5 levels, which then can be split by spin-orbit coupling or an additional low-symmetry crystal-field component originating from a cooperative JT distortion.<sup>5,17</sup> Goodenough pointed out that in case the octahedral-site cations do not contribute to the elastic anisotropy, then the elastic energy may be too small to include a static Jahn-Teller distortion but in case a distortion occurs, it is of tetragonal (c/a<1) symmetry.<sup>5</sup> In FeCr<sub>2</sub>S<sub>4</sub> magnetic order, driven by the strong FM Cr-Cr exchange, occurs close to T<sub>c</sub>=180 K.<sup>6</sup> Via an antiferromagnetic coupling of the Fe sublattice to the Cr moments, ferrimagnetic order is established at the magnetic phase transition. From neutron powder diffraction at 4.2 K, it has been concluded that the compound remains cubic down to low temperatures and that the spin arrangement is of a

simple collinear ferrimagnetic type.<sup>7</sup> The observed magnetic intensities can well be described assuming  $\mu_{\text{Cr}}=2.9\mu_{\text{B}}$  and  $\mu_{\text{Fe}}=4.2\mu_{\text{B}}$ . The former is close to the spin-only value of  $\text{Cr}^{3+}$  and the latter is slightly enhanced due to moderate spin-orbit coupling.

Early on, there have been a number of Mössbauer studies on  $\text{FeCr}_2\text{S}_4$  reporting the observation of a nonzero quadrupole shift of the hyperfine pattern indicating substantial deviations from cubic symmetry at the tetrahedral *A* sites.<sup>8–11</sup> This has been explained by the concept of magnetically induced electric field gradients or by the appearance of magnetostriction effects. Spender and Morrish proposed that the finite electric field gradient arises from a Jahn-Teller stabilization of the  ${}^5\text{E}_g$  ground state of  $\text{Fe}^{2+}$  in tetrahedral symmetry which appears close to the orbital-order transition at  $T_{\text{oo}}=10$  K.<sup>11</sup> They concluded that  $\text{FeCr}_2\text{S}_4$  may be one of the rare examples which allow studying the transition from a dynamic to a static JT effect. Later on, this proposal has been substantiated by further Mössbauer<sup>12,13</sup> and low-temperature heat-capacity experiments.<sup>13</sup> The heat-capacity experiments in pure and doped compounds documented the extreme dependence of the appearance of a static JT transition on details of stoichiometry.<sup>13</sup> The sensitivity of the onset of orbital order has been further elucidated by detailed experiments on single crystals and polycrystals depending on the conditions of synthesis.<sup>14</sup>

Since then, the anomaly at 10 K in  $\text{FeCr}_2\text{S}_4$  has been lively debated<sup>15–17</sup> and described as a cooperative JT transition caused by an antiferrodistortive coupling between the Jahn-Teller ions.<sup>17</sup> In Ref. 17, Feiner has shown that fitting of Mössbauer data reveals slightly enhanced orbital-ordering temperatures (13–17 K) while the thermodynamic transition appears close to 9 K. In addition, he deduced the splitting  $\Delta=17(2)$   $\text{cm}^{-1}$  between the ground and the first excited vibronic states and concluded that the chromium E phonon modes are coupled most strongly to the cooperative JT effect.<sup>17</sup> Later on, it has been documented by dielectric spectroscopy that the orbital degrees of freedom in single-crystalline  $\text{FeCr}_2\text{S}_4$  undergo a glassy freezing<sup>18</sup> and the question has been raised if the purely stoichiometric compound reveals long-range orbital order or a frustrated orbital ground state with local OO only. Furthermore, based on electron-spin-resonance studies,<sup>19</sup> on magnetic dc and ac susceptibility measurements,<sup>20,21</sup> ultrasonic studies,<sup>22</sup> and transmission-electron microscopy<sup>23</sup> experimental evidence has been provided that in  $\text{FeCr}_2\text{S}_4$ , a further phase transition exists for temperatures close to 60 K. A symmetry reduction from cubic to triclinic, reentrant spin-glass behavior or magnetic domain reorientation processes have been proposed to explain these unusual observations. In contradiction, more recent single-crystal x-ray diffraction (XRD) experiments at low temperatures found no indications of any structural phase transition down to the lowest temperatures and reported a simple cubic spinel structure even at 4 K.<sup>24</sup> In recent Raman-scattering investigations, the observed number of modes also agrees with this structure. However, three of the four allowed modes show a continuous softening for temperatures below  $T_c$  without saturation to lowest temperature. Furthermore, a broad one-magnon excitation vanishes already at  $0.83T_c$ . Also this observation is taken as evidence for magnetic

fluctuations.<sup>25</sup> Recently, detailed muon-spin rotation ( $\mu\text{SR}$ ) experiments<sup>26</sup> provided experimental evidence that on decreasing temperatures close to 60 K, the ferrimagnetic structure evolves into an incommensurate, nonsinusoidally modulated spin structure which then remains the stable spin configuration down to the lowest temperatures even in the orbitally ordered state. In addition, during the last decade, the scientific interest on  $\text{FeCr}_2\text{S}_4$  gained further momentum triggered by reports of colossal magnetoresistance effects in pure and copper-doped compounds.<sup>27,28</sup>

This work aims to determine the electronic ground state of  $\text{FeCr}_2\text{S}_4$  and to establish the correlations between structural, magnetic, and orbital degrees of freedom in this compound. To resolve this long-standing problem, we performed high-resolution x-ray synchrotron powder-diffraction, magnetic-susceptibility, sound-velocity, thermal-expansion, and heat-capacity experiments. We focus on polycrystalline samples which can be synthesized close to ideal stoichiometry. In the course of this work on single-crystalline and polycrystalline material of the title compound, we have found that  $\text{FeCr}_2\text{S}_4$  single crystals grown by chemical transport can be prepared impurity free using bromine gas as transport agent but are slightly electronically doped when using chlorine gas instead, however the former are rather limited in size. Hence we concentrated on the polycrystalline material throughout this work.

## II. EXPERIMENTAL DETAILS

Polycrystalline samples of  $\text{FeCr}_2\text{S}_4$  were prepared by solid-state reaction using high-purity elements. To reach complete reaction, the synthesis was repeated several times with respective regrinding and pressing of the materials. Annealing in chalcogen atmosphere and/or vacuum was utilized for a variation in the sample stoichiometry. This allows to tune the anomaly at around 10 K related to orbital ordering as shown in Ref. 29. Wavelength-dispersive x-ray electron-probe analysis (Camebacs SX 50) was used to determine the sample composition. The microprobe analysis showed that the sample with the most pronounced low-temperature anomaly has a purely stoichiometric ratio of Fe/Cr/S. For preparation of dense samples suitable for ultrasound and optical studies, we used the spark plasma sintering (SPS) technique similar to that described in Ref. 30. As starting materials for SPS, we utilized iron sulfide and chromium sulfide prepared by solid-state synthesis that allowed to avoid oxygen contamination observed when using industrial binary sulfides.<sup>30</sup> X-ray powder analysis of crashed polycrystalline and SPS samples show identical diffraction patterns corresponding to the pure spinel phase without any notable impurities.

High-resolution x-ray powder diffraction has been performed at the Swiss Light Source Materials Science beamline powder-diffraction station. The incoming x-ray wavelength of  $\lambda=0.618049$  Å, as determined using a silicon standard, allowed to reach  $2 \sin \theta/\lambda=2.22$  Å<sup>-1</sup>. The sample has been loaded in a 0.5 mm quartz capillary in a Janis He cryostat and XRD patterns have been collected in a temperature range from 5 to 180 K. Structure and microstructure

refinement have been performed by Rietveld technique utilizing the FULLPROF suite.<sup>31</sup> The dc magnetic susceptibility has been studied utilizing a commercial superconducting quantum interference device magnetometer (Quantum Design MPMS-5). Sound-velocity experiments were performed using a phase-sensitive setup in the temperature range 4–300 K. For generation and detection of the ultrasound waves, LiNbO<sub>3</sub> transducers were used with a fundamental frequency of 10 MHz. The thermal-expansion experiments were carried out in a homebuilt setup using a capacitance bridge which works for temperatures from 1.5 to 300 K and in external magnetic fields up to 16 T. The heat capacity was measured in a physical properties measurements system (PPMS, Quantum Design) for temperatures between 1.8 K and room temperature.

### III. RESULTS AND DISCUSSION

We performed high-resolution diffraction experiments with particular attention to the temperature range at around 60 K and around 10 K since conventional diffraction techniques did not find any deviation from the cubic spinel structure of FeCr<sub>2</sub>S<sub>4</sub> even at low temperatures. In any case, one would expect that the onset of long-range orbital order has to be accompanied by a structural anomaly. At 180 K, we determined a lattice constant  $a=9.9894(3)$  Å. We found an appreciable contraction of the lattice on cooling which levels off below 60 K reaching a constant value toward the lowest temperatures in general agreement with results of Ref. 24. At 5 K, the lattice constant has a value  $a=9.9808(3)$  Å and the cubic normal spinel structure fits well the low-temperature diffraction pattern.

However, we observe a broadening of all Bragg reflections at low temperatures, which is rather small and, therefore, could not be detected in previous diffraction experiments. The onset of this broadening coincides with the spin-reorientation transition at around 60 K and shows a maximum close to the orbital ordering transition at 10 K, as illustrated in Fig. 1. To our opinion, this broadening is a signature of the splitting of Bragg reflections which, however, cannot be resolved even in this high-resolution experiment. Although the refinement of the structural data has been performed in cubic symmetry and therefore their physical relevance is limited, we want to point out that the thermal displacement parameters  $\beta_{ii}$  ( $\beta_{11}=\beta_{22}=\beta_{33}$ ) for iron, chromium, and sulfur ions qualitatively trace the changes in lattice symmetry with temperature (shown as an inset of Fig. 1). All ions reveal a striking anomaly of their thermal parameters, with a maximum at 15 K, slightly above the orbital-order transition suggesting the temperature range of the strongest orbital and lattice fluctuations. The displacement parameters are largest for iron and smallest for chromium. As we measured strictly elastic scattering due to the presence of analyzers in the beamline, this anomaly in the displacements of all ions points toward cooperative Jahn-Teller distortions. It also seems natural that the ions which are involved in the Jahn-Teller complex, namely, JT-active Fe<sup>2+</sup> including the neighboring sulfur ions exhibit the highest thermal displacement parameters while the chromium ions are much less in-

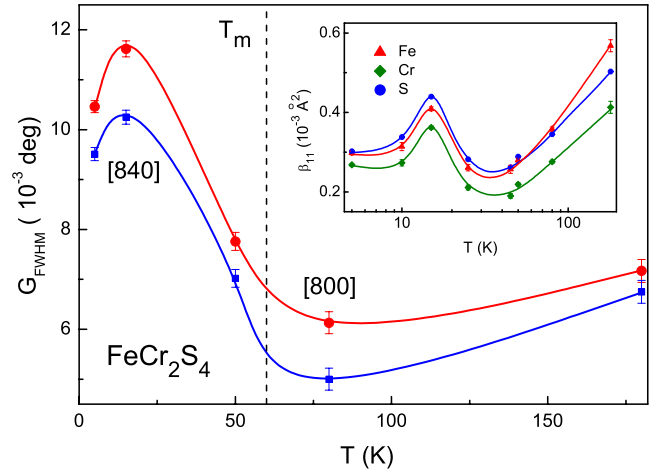


FIG. 1. (Color online) Temperature dependence of the linewidth of the Gaussian contribution to the [800] and [840] Bragg peaks. Inset: temperature dependence of the displacement parameters  $\beta_{ii}$  of Fe (red triangles), Cr (green rhombs), and S (blue circles) from the high-resolution diffraction data. Lines through the data points are guide to the eyes.

involved but still reveal a clear anomaly in the vicinity of the orbital-order transition. This observation agrees with Goodenough's proposal that the two empty orbitals of Cr are directed toward the nearest-neighbor anions and participate in coordinate covalence.<sup>5</sup> This effect stabilizes the Cr in its octahedral environment but enhances the JT anisotropy of tetrahedral Fe<sup>2+</sup>. The anomaly in the temperature dependence of the Cr mean-square displacements also agrees with Feiner's proposal that the chromium E modes are strongly involved in the cooperative JT transition.<sup>17</sup>

These structural anomalies also show up in the thermal-expansion measurements performed in the SPS ceramic sample below the magnetic ordering temperature depicted in Fig. 2, where the normalized change in sample length  $\Delta L/L_0$  is plotted for temperatures between 4 and 160 K. Here  $L_0$  is the sample length at 4 K. The figure documents a smooth

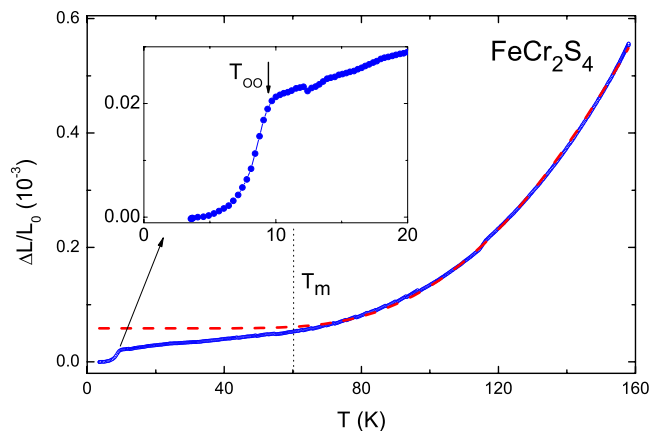


FIG. 2. (Color online) Normalized thermal expansion ( $\Delta L/L_0$ ) vs temperature in FeCr<sub>2</sub>S<sub>4</sub> (closed blue circles). The dashed line corresponds to a fit with a behavior of a normal anharmonic solid as described in the text. The inset shows an enlarged region of the thermal expansion around the orbital-ordering temperature.

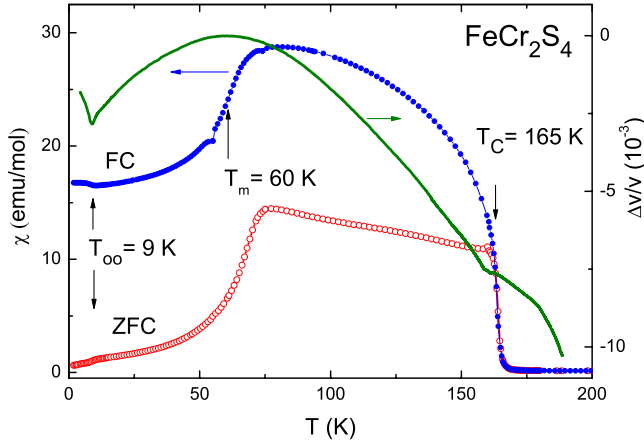


FIG. 3. (Color online) Left scale: temperature dependence of zero-field-cooled (open red circles) and field-cooled (closed blue circles) susceptibility  $\chi = M/H$  of  $\text{FeCr}_2\text{S}_4$  in an external magnetic field  $H = 100$  Oe. Right scale: temperature dependence of the relative change in the longitudinal sound velocity (solid green line). This line corresponds to an averaged change in the sound velocity as measured in heating and cooling cycles. The characteristic temperatures are indicated by vertical arrows.

decrease in the sample length on decreasing temperature as expected for a normal anharmonic solid. A clear anomaly at the orbital-ordering temperature (see inset for an enlarged view) signals a contraction of the lattice in agreement with an antiferrodistortive arrangement of the  $\text{FeS}_4$  tetrahedra in the ground state. The onset of orbital order can be pinned down to a temperature of 9.2 K and the transition clearly looks like a smooth second-order transition, which is further supported by the fact that we were not able to detect any hysteresis effects.

The temperature-dependent change in sample length between 60 and 160 K is well described using a fit according to  $L(T) = L_0(1 + A/[\exp(\theta/T) - 1])$ , where  $L_0$  is the sample length extrapolated toward 0 K,  $\theta$  is an averaged Debye temperature, and  $A$  is a fitting constant. From the fit, we estimated an approximate Debye temperature of  $\theta = 507$  K. Below 60 K, the thermal-expansion data starts to deviate from the extrapolated curve for a normal anharmonic solid coinciding with the broadening of the Bragg peaks. The enhanced shrinking of the lattice below 60 K can then be understood due to the onset of short-range orbital ordering.

Further evidence for this scenario is shown in Fig. 3 where ultrasound data (right scale) are shown together with the magnetic susceptibility (left scale). In the latter, a clear signature of the ferrimagnetic transition with a significant onset of spontaneous magnetization can be noticed. From a detailed analysis of the magnetization around the magnetic ordering temperature, utilizing Arrott plots, and critical-scaling analysis, we determined a transition temperature of 165 K. In literature, there exists a large spread of reported magnetic transitions in  $\text{FeCr}_2\text{S}_4$  on the order of  $\Delta T_C = 15$  K, which probably results from details of the sample preparation, sample stoichiometry, and how the magnetic ordering temperature is determined. Just below  $T_C$ , field-cooled (FC) and zero-field-cooled (ZFC) susceptibility separate, a fact that can be attributed to magnetic domain dynamics as estab-

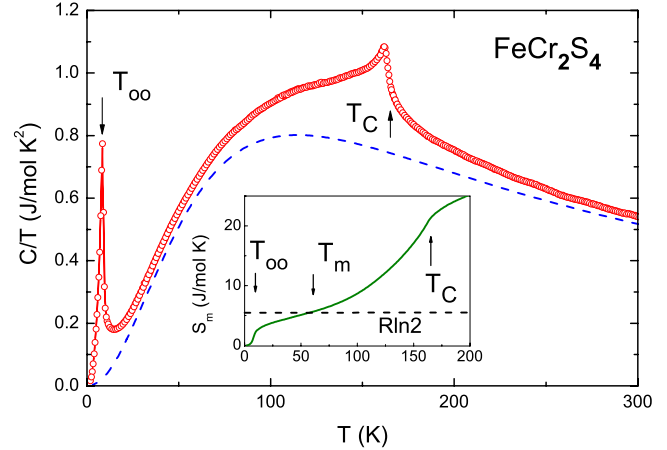


FIG. 4. (Color online) Heat capacity of  $\text{FeCr}_2\text{S}_4$  in representation  $C/T$  vs  $T$  (red open circles). The characteristic temperatures of the orbital-ordering transition at  $T_{oo}$ , of the anomaly at  $T_m$ , and of the long-range ferrimagnetic order at  $T_C$  are indicated by arrows. The simulated lattice contribution is shown by a blue dashed line. Inset: magnetic entropy determined after subtraction of the lattice contribution.

lished by ac susceptibility studies.<sup>20</sup> However, both ZFC and FC susceptibilities reveal a strong continuous decrease close to 60 K signaling significant changes in the long-range ordered magnetic structure. A further small kink appears at approximately 9 K associated with the onset of long-range orbital order via the cooperative JT effect.

Turning to the longitudinal sound velocity in the dense SPS ceramic sample, we plotted the changes in sound velocity  $\Delta v/v$  normalized to its maximum value. On decreasing temperatures, from 200 to 60 K we find an overall increase in the sound velocity in agreement with measurements on a single-crystalline sample.<sup>22</sup> This increase roughly resembles the expectations of the temperature dependence of the velocity of sound in anharmonic solids and agrees with the observed behavior of the thermal expansion. A small dip close to 160 K signals the onset of ferrimagnetic order. Obviously, magnetic exchange and the onset of spin order are only very weakly coupled to the lattice and specifically to the acoustic modes. However, at 60 K the sound velocity exhibits a maximum and decreases toward lower temperatures indicating a softening of acoustic lattice vibrations concomitantly to the anomalous broadening of the Bragg reflections. This softening continues down to the orbital-ordering temperature  $T_{oo}$  and then increases again in the orbitally ordered state. Such a behavior has often been observed in Jahn-Teller systems and documents the strong coupling of strain fields to the orbital degrees of freedom.<sup>3</sup> Note, however, that we measure the longitudinal sound velocity of an effective medium averaging over all elastic modes and ultrasound studies on single crystals along different crystallographic directions are necessary which would provide useful information on the symmetry of the induced distortions and on the low-temperature structure.

Finally, we show the temperature dependence of the specific heat divided by temperature  $C/T$  in  $\text{FeCr}_2\text{S}_4$  in Fig. 4. In this representation, the lattice contribution to the specific

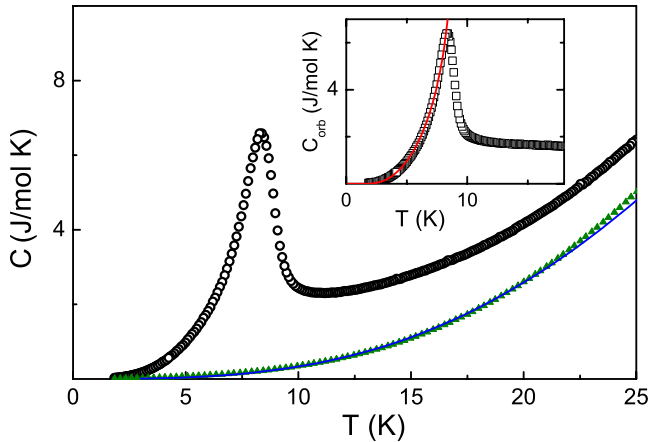


FIG. 5. (Color online) Heat capacity of  $\text{FeCr}_2\text{S}_4$  at low temperatures (open circles). The green triangles show the heat capacity of  $\text{Fe}_{0.5}\text{Cu}_{0.5}\text{Cr}_2\text{S}_4$ . The blue solid line is a fit describing the lattice contribution (see text). The inset shows the heat capacity solely derived from the orbital degrees of freedom. Here the phonon contribution as indicated in the main frame has been subtracted. The red solid line is a mean-field fit as described in the text utilizing a mean-field gap of 14.8 K.

heat  $C_{\text{lat}}/T$  (dashed line) exhibits a maximum at elevated temperatures. The lattice contribution  $C_{\text{lat}}$  was fitted by 1 Debye term with the Debye temperature of 180 K and three Einstein terms with Einstein temperatures of 220 K, 320 K, and 530 K, respectively. These fit parameters were proved using  $\text{ZnCr}_2\text{S}_4$  and  $\text{ZnAl}_2\text{S}_4$  as reference spinel compounds which show very similar phononic spectra as  $\text{FeCr}_2\text{S}_4$ . Two well-defined anomalies are superimposed on this phonon-derived contribution. The upper anomaly at  $T_C = 165$  K corresponds to the onset of spin order. The lower anomaly close to 10 K is due to the cooperative JT transition with the onset of the long-range orbital order. This is corroborated by the temperature dependence of the magnetic entropy  $S_m$  determined from the integral over  $(C - C_{\text{lat}})/T$ , which exhibits two pronounced steps at the corresponding transitions as shown in the inset of Fig. 4. At the orbital-order transition, the entropy reaches about 50% of  $R \ln 2$  expected for the orbital doublet. The full entropy of the orbital doublet is reached only at about 60 K confirming our scenario of the onset of short-range orbital correlations at this temperature. At the spin-ordering temperature, again only about 50% of the full spin entropy  $R(2 \ln 4 + \ln 5)$  is reached, indicating the importance of strong spin correlations in the paramagnetic regime in agreement with the large negative Curie-Weiss temperature of about 350 K. We want to emphasize that no distinct anomaly in the specific heat can be detected close to 60 K, i.e., that no order-disorder transition takes place at this temperature but the onset of short-range orbital order seems to alter the existing long-range spin ordering resulting in the decrease in the susceptibility shown in Fig. 3. This transition is connected with a small change in entropy only and cannot be separated from the spin and lattice contributions.

Further analysis of the low-temperature specific heat is given in Fig. 5. The important problem here is to correctly evaluate the lattice and magnon contributions. As an independent check for these contributions, we used the specific-

heat data of the isostructural reference spinel compound  $\text{Fe}_{0.5}\text{Cu}_{0.5}\text{Cr}_2\text{S}_4$  shown by triangles in Fig. 5.  $\text{Fe}_{0.5}\text{Cu}_{0.5}\text{Cr}_2\text{S}_4$  exhibits rather similar phonon spectra<sup>32</sup> and similar ferrimagnetic behavior as  $\text{FeCr}_2\text{S}_4$  but in contrast to  $\text{FeCr}_2\text{S}_4$  does not show any cooperative Jahn-Teller transition. We observed that at temperatures below 20 K, the specific heat of  $\text{Fe}_{0.5}\text{Cu}_{0.5}\text{Cr}_2\text{S}_4$  is very close to the phonon specific heat estimated above which is shown by the blue solid line. This additionally justifies the correctness of our modeling of the lattice specific heat for pure compound and indicates that magnon contribution is negligible at least in the range of the low-temperature transition.

In the inset of Fig. 5, we provide a more detailed analysis of the lambda-like anomaly observed at the JT transition. This inset shows the Jahn-Teller-derived excess heat capacity of  $\text{FeCr}_2\text{S}_4$  plotted as  $C_{\text{orb}}$  vs  $T$ , after subtracting the phonon contribution as documented in the main frame of Fig. 5. To describe the residual heat capacity below  $T_{\text{oo}}$ , we use a mean-fieldlike approach for a two-level system, where a gap  $\Delta$  is opened at  $T_{\text{oo}}$  providing a steplike increase in the specific heat at the ordering temperature and an exponential decrease toward 0 K. We assume that the temperature dependence of the gap follows  $\Delta(T)/\Delta_0 = \tanh(\Delta T_{\text{oo}}/\Delta_0 T)$ , where  $\Delta_0$  denotes the gap value at 0 K (in units of temperature).<sup>33</sup> This behavior has been derived for system of ferromagnetically coupled spins with  $S = \frac{1}{2}$ . Using this formalism, the transition temperature is given by  $T_{\text{oo}} = \Delta_0/2$  and the steplike jump at the ordering temperature in the heat capacity amounts to  $1.5R$ , where  $R$  is the gas constant. Indeed, in the most stoichiometric polycrystalline sample, this value is clearly reached<sup>29</sup> confirming the validity of the mean-field description used here. Utilizing this temperature-dependent gap, we calculated the orbital-derived heat capacity of  $\text{FeCr}_2\text{S}_4$  using  $C_{\text{orb}}(T) = C_0 \exp(-\Delta/T)$ . Fixing the orbital-order transition to 9 K, we find a gap  $\Delta_0 = 14.8$  K  $\sim 10.3$   $\text{cm}^{-1}$ . For the most stoichiometric sample, the gap value  $\Delta_0$  is 18.3 K  $\sim 12.7$   $\text{cm}^{-1}$ .

This value is surprisingly close to the splitting of the ground state of isolated  $\text{Fe}^{2+}$  ions in an insulating matrix due to spin-orbit coupling. In second-order spin-orbit coupling, the  ${}^5\text{E}$  ground state is split into five equally spaced levels with an energy separation of approximately 10–20  $\text{cm}^{-1}$ . For example, Slack *et al.*<sup>34</sup> determined a splitting of the ground state of  $\text{Fe}^{2+}$  at the tetrahedral site of the spinel  $\text{MgAl}_2\text{O}_4$  on the order of 13(2)  $\text{cm}^{-1}$ . With respect to a temperature scale, this splitting corresponds to approximately 20 K. In the heat capacity, the level splitting should be detectable as a pronounced Schottky-type anomaly which would be clearly visible already at temperatures  $T > T_{\text{oo}}$ . However, our experimental data fully exclude this effect indicating very low value of splitting. Concomitantly, the steplike increase in the heat capacity at the JT transition would be reduced,<sup>35</sup> which also seems not to be the case. An explanation of this low value of the ground-state splitting of the  $\text{Fe}^{2+}$  ions in the title compound as compared to isolated iron ions which are tetrahedrally coordinated can only be provided assuming that in the orbitally disordered phase, a dynamic Jahn-Teller effect reduces the splitting considerably.

The low-lying excitations and the energy levels of  $\text{Fe}^{2+}$  ions in tetrahedral environment have been treated by various

authors.<sup>3,5,16,17</sup> A unified description of diluted Fe<sup>2+</sup> ions in CoCr<sub>2</sub>S<sub>4</sub> and the cooperative Jahn-Teller system FeCr<sub>2</sub>S<sub>4</sub> has been proposed in a mean-field approach by Feiner in Ref. 17. In this scenario, the interplay of spin-orbit coupling, the vibronic interaction of the FeS<sub>4</sub> tetrahedra via E-type lattice vibrations, and the antiferrodistortive coupling to neighboring tetrahedra give rise to a phase diagram where a second-order phase transition from a high-temperature paradistortive phase (dynamic Jahn-Teller effect) to a low-temperature pseudospin-flop phase (static cooperative Jahn-Teller distortion) can occur. This transition is accompanied by an abrupt change in the ground-state orbital wave function and the splitting of the lowest-lying vibronic doublet shows an order parameter like increase below the Jahn-Teller transition. The estimated value  $\Delta=17\text{ cm}^{-1}$  for the splitting roughly agrees with the value obtained from our specific-heat data.

#### IV. CONCLUDING REMARKS

In this paper, we present a detailed structural, magnetic, and thermodynamic study of the orbital order in FeCr<sub>2</sub>S<sub>4</sub> for temperatures close to 10 K and a further transition at 60 K. The following main conclusions can be drawn: (i) in the high-resolution x-ray diffraction, we observed a considerable broadening of the diffraction lines that sets in at around 60 K and reaches a maximum at  $T_{oo}$  evidencing the structural anomalies at these temperatures. This broadening is interpreted as a signature of splitting of Bragg reflections which, however, cannot be resolved even in this high-resolution experiment. The changes are rather subtle and therefore at low temperatures ( $T < T_{oo}$ ), the structure still can be refined using cubic symmetry. However, close to the orbital-order transition, we find a clear peak in the temperature dependence of the mean-square displacements for all ions, with the strongest effect for iron and the weakest for chromium ions.

(ii) The temperature-dependent magnetic susceptibility reveals a strong anomaly at 60 K, which in the light of recent  $\mu$ SR experiments<sup>26</sup> is interpreted as a spin-reorientation anomaly. Here the collinear ferrimagnetic phase which is established at the magnetic ordering transition at 165 K transforms into a noncollinear helical structure below 60 K. The

entropy of this transformation related to a spin rearrangement is very weak and therefore is not evidenced in the heat-capacity experiments.

(iii) From ultrasound experiments, we conclude that short-range orbital ordering starts at 60 K and possibly induce the magnetic transition at 60 K. These strong fluctuations apparently dominate all Mössbauer experiments reported so far.<sup>8–11</sup> All these experiments report on the observation of significant nonzero quadrupole shifts obviously induced by orbital fluctuations and local dynamic deviations from cubic symmetry.

(iv) From thermal expansion, we find normal anharmonic behavior at temperatures between 300 and 60 K. Below 60 K, a pronounced deviation from the normal anharmonic behavior is observed. These observations compare well to earlier Raman-scattering data.<sup>25</sup> A significant drop in  $\Delta L/L_o$  at the orbital-order transition  $T_{oo}$  indicates that the lattice is strongly involved in the cooperative Jahn-Teller effect.

(v) We provide a detailed analysis of the low-temperature heat capacity. The lambda anomaly at the JT transition can be satisfactorily described with a mean-field gap  $\Delta = 18.3\text{ K} \sim 12.7\text{ cm}^{-1}$ , which is close to the expected value of  $2T_{oo}$  within the mean-field model of an effective spin  $\frac{1}{2}$ . This value is in rough agreement with the estimate  $\Delta = 17\text{ cm}^{-1}$  derived from a vibronic coupling approach to the phase transition.

Thus, our study provides clear experimental evidence of structural anomaly that accompany the low-temperature transition at around 10 K in FeCr<sub>2</sub>S<sub>4</sub>. Moreover, we propose that the spin-reorientation transition at 60 K, which is clearly observed by our structurally sensitive experimental techniques, is directly related to the enhanced structural and orbital fluctuations.

#### ACKNOWLEDGMENTS

The authors thank Dana Vieweg and Thomas Wiedenmann for experimental support. This research has been supported by the DFG via TRR 80 (Augsburg—Munich). The support of DFG via Grant No. LE 967/6-1 (Braunschweig) is also gratefully acknowledged.

<sup>1</sup>Y. Tokura and N. Nagaosa, *Science* **288**, 462 (2000).

<sup>2</sup>H. A. Jahn and E. Teller, *Proc. R. Soc. London, Ser. A* **161**, 220 (1937).

<sup>3</sup>For a review see, G. A. Gehring and K. A. Gehring, *Rep. Prog. Phys.* **38**, 1 (1975).

<sup>4</sup>K. I. Kugel' and D. I. Khomskii, *Sov. Phys. Usp.* **25**, 231 (1982).

<sup>5</sup>J. F. Goodenough, *J. Phys. Chem. Solids* **25**, 151 (1964).

<sup>6</sup>F. K. Lotgering, *Philips Res. Rep.* **11**, 190 (1956).

<sup>7</sup>G. Shirane, D. E. Cox, and S. J. Pickart, *J. Appl. Phys.* **35**, 954 (1964).

<sup>8</sup>G. H. Hoy and S. Chandra, *J. Chem. Phys.* **47**, 961 (1967).

<sup>9</sup>M. Eibschütz, S. Shtrikman, and Y. Tenenbaum, *Phys. Lett.* **24**, 563 (1967).

<sup>10</sup>G. M. Hoy and K. P. Singh, *Phys. Rev.* **172**, 514 (1968).

<sup>11</sup>M. R. Spender and A. H. Morrish, *Solid State Commun.* **11**, 1417 (1972).

<sup>12</sup>A. M. van Diepen and R. P. van Staple, *Solid State Commun.* **13**, 1651 (1973).

<sup>13</sup>F. K. Lotgering, A. M. van Diepen, and J. F. Olijhoek, *Solid State Commun.* **17**, 1149 (1975).

<sup>14</sup>V. Tsurkan, H.-A. Krug von Nidda, A. Krimmel, P. Lunkenheimer, J. Hemberger, T. Rudolf, and A. Loidl, *Phys. Status Solidi A* **206**, 1082 (2009).

<sup>15</sup>L. Brossard, J. L. Dormann, L. Goldstein, P. Gibart, and P. Renaudin, *Phys. Rev. B* **20**, 2933 (1979).

<sup>16</sup>L. F. Feiner and R. P. van Staple, *Phys. Rev. B* **22**, 2585 (1980).

<sup>17</sup>L. F. Feiner, *J. Phys. C* **15**, 1515 (1982).

- <sup>18</sup>R. Fichtl, V. Tsurkan, P. Lunkenheimer, J. Hemberger, V. Fritsch, H.-A. Krug von Nidda, E.-W. Scheidt, and A. Loidl, *Phys. Rev. Lett.* **94**, 027601 (2005).
- <sup>19</sup>V. Tsurkan, M. Lohmann, H.-A. Krug von Nidda, A. Loidl, S. Horn, and R. Tidecks, *Phys. Rev. B* **63**, 125209 (2001).
- <sup>20</sup>V. Tsurkan, M. Baran, R. Szymczak, H. Szymczak, and R. Tidecks, *Physica B* **296**, 301 (2001).
- <sup>21</sup>V. Tsurkan, J. Hemberger, M. Klemm, S. Klimm, A. Loidl, S. Horn, and R. Tidecks, *J. Appl. Phys.* **90**, 4639 (2001).
- <sup>22</sup>D. Maurer, V. Tsurkan, S. Horn, and R. Tidecks, *J. Appl. Phys.* **93**, 9173 (2003).
- <sup>23</sup>M. Mertinat, V. Tsurkan, D. Samusi, R. Tidecks, and F. Haider, *Phys. Rev. B* **71**, 100408(R) (2005).
- <sup>24</sup>L. L. Presti, D. Invernizzi, R. Soave, and R. Destro, *Chem. Phys. Lett.* **416**, 28 (2005).
- <sup>25</sup>K.-Y. Choi, P. Lemmens, P. Scheib, V. Gnezdilov, Yu. G. Pashkevich, J. Hemberger, A. Loidl, and V. Tsurkan, *J. Phys.: Condens. Matter* **19**, 145260 (2007).
- <sup>26</sup>G. M. Kalvius, A. Krimmel, O. Hartmann, R. Wäppling, F. E. Wagner, F. J. Litterst, V. Tsurkan, and A. Loidl, *J. Phys.: Condens. Matter* **22**, 052205 (2010).
- <sup>27</sup>A. P. Ramirez, R. J. Cava, and J. Krajewski, *Nature (London)* **386**, 156 (1997).
- <sup>28</sup>V. Fritsch, J. Deisenhofer, R. Fichtl, J. Hemberger, H.-A. Krug von Nidda, M. Mücksch, M. Nicklas, D. Samusi, J. D. Thompson, R. Tidecks, V. Tsurkan, and A. Loidl, *Phys. Rev. B* **67**, 144419 (2003).
- <sup>29</sup>V. Tsurkan, V. Fritsch, J. Hemberger, H.-A. Krug von Nidda, D. Samusi, S. Körner, E.-W. Scheidt, S. Horn, R. Tidecks, and A. Loidl, *J. Phys. Chem. Solids* **66**, 2036 (2005).
- <sup>30</sup>V. Zestrea, V. Y. Kodash, V. Felea, P. Petrenco, D. V. Quach, J. R. Groza, and V. Tsurkan, *J. Mater. Sci.* **43**, 660 (2008).
- <sup>31</sup>J. Rodríguez-Carvajal, *Physica B* **192**, 55 (1993).
- <sup>32</sup>T. Rudolf, K. Pucher, F. Mayr, D. Samusi, V. Tsurkan, R. Tidecks, J. Deisenhofer, and A. Loidl, *Phys. Rev. B* **72**, 014450 (2005).
- <sup>33</sup>A. H. Cooke, S. J. Swithenby, and M. R. Wells, *Solid State Commun.* **10**, 265 (1972).
- <sup>34</sup>G. A. Slack, F. S. Ham, and R. M. Chrenko, *Phys. Rev.* **152**, 376 (1966).
- <sup>35</sup>B. S. Lee, *J. Low Temp. Phys.* **13**, 81 (1973).